

## Molecular Crystals and Liquid Crystals

Publication details, including instructions for authors and subscription information:

<http://www.tandfonline.com/loi/gmcl20>

### Measurement of Azimuthal Backflow in a Dual-Frequency Chiral HAN Cell

S. A. Jewell<sup>a</sup> & J. R. Sambles<sup>a</sup>

<sup>a</sup> Thin Film Photonics Group, School of Physics, University of Exeter, Exeter, UK

Version of record first published: 22 Sep 2010

To cite this article: S. A. Jewell & J. R. Sambles (2007): Measurement of Azimuthal Backflow in a Dual-Frequency Chiral HAN Cell, *Molecular Crystals and Liquid Crystals*, 477:1, 57/[551]-65/[559]

To link to this article: <http://dx.doi.org/10.1080/15421400701675382>

PLEASE SCROLL DOWN FOR ARTICLE

Full terms and conditions of use: <http://www.tandfonline.com/page/terms-and-conditions>

This article may be used for research, teaching, and private study purposes. Any substantial or systematic reproduction, redistribution, reselling, loan, sub-licensing, systematic supply, or distribution in any form to anyone is expressly forbidden.

The publisher does not give any warranty express or implied or make any representation that the contents will be complete or accurate or up to date. The accuracy of any instructions, formulae, and drug doses should be independently verified with primary sources. The publisher shall not be liable for any loss, actions, claims, proceedings, demand, or costs or damages

whatsoever or howsoever caused arising directly or indirectly in connection with or arising out of the use of this material.

## Measurement of Azimuthal Backflow in a Dual-Frequency Chiral HAN Cell

S. A. Jewell

J. R. Sambles

Thin Film Photonics Group, School of Physics, University of Exeter,  
Exeter, UK

*An optical characterization technique has been used to determine the response of a chiral dual-frequency hybrid aligned nematic liquid crystal cell to a multiple frequency pulse. The cell goes from homeotropic to twisted homogeneous alignment when the frequency of an applied voltage is switched from below to above the cross-over frequency of the material. Analysis of the response of the director reveals a new form of backflow which arises due to a coupling between the rotation and flow of the liquid crystal. The results show good agreement with modelled profiles generated using the Leslie-Ericksen-Parodi nematodynamics theory.*

**Keywords:** backflow; cholesteric; dual-frequency; hybrid aligned

### I. INTRODUCTION

The limiting factor in the switching speed of pixels in a nematic liquid crystal display is the relatively slow response of the director to the removal of a voltage. In contrast, high switch-on speeds are achievable by driving the pixel into the on-state by the application of an electric field, but the switch-off time is dictated by the mechanical and viscous forces acting on the material. The use of a dual-frequency nematic liquid crystal may go some way to solving this problem [1,2]. These materials have highly frequency-dependent dielectric anisotropies

The authors would like to thank Dr. C. V. Brown of Nottingham Trent University, UK for the dielectric anisotropy and elastic constant measurements. This project forms part of a COMIT Faraday partnership funded by the Engineering and Physical Sciences Research Council and the DTI.

Address correspondence to Dr Sharon A Jewell, Thin Film Photonics Group, School of Physics, University of Exeter, Stocker Road, Exeter, EX4 4QL, UK. E-mail: s.a.jewell@exeter.ac.uk

where  $\Delta\varepsilon (= \varepsilon_{\parallel} - \varepsilon_{\perp})$  can be positive or negative depending on the frequency chosen where a cross-over frequency,  $f_{co}$  is defined as the frequency at which  $\Delta\varepsilon = 0$  (i.e.  $\varepsilon_{\parallel} = \varepsilon_{\perp}$ ). These materials can therefore be driven into an alignment either parallel or perpendicular to the direction of the applied field by simply changing the frequency of the voltage applied.

Previous work examining the dynamic properties of hybrid aligned nematic (HAN) cells has demonstrated that they have the potential for fast switching between homeotropic and homogeneous alignments. This arises due to the aligning layers providing an equal bias towards the two types of alignment, resulting in thresholdless switching [3]. However, this structure is of limited use in a display as the transmission of light through the cell when it is homogeneously aligned is purely dictated by the optical birefringence of the material, which may not be sufficient for a high quality contrast ratio. The amount of light transmitted in the homogeneous (high frequency) state can be improved by adding a chiral dopant to the dual-frequency liquid crystal to produce a pitch which is comparable to four times the thickness of the cell to induce a  $90^\circ$  twist through the cell. The azimuth is dictated by the homogeneous alignment on one surface and the twist is unrestricted at the homeotropic surface, allowing the material to form a relatively unconstrained twist state [4]. For a suitably low concentration of chiral dopant, the material maintains its dual-frequency properties, and so the structure can be switched from the 0 V chiral HAN (CHAN) structure (which both twists and tilts though approximately  $90^\circ$ ) into either a homeotropically aligned state at low frequencies ( $f < f_{co}$ ) or into a twisted homogeneous state of pitch comparable to the natural pitch of the material at high frequencies (Fig. 1). By applying a low-frequency pulse to switch the cell to homeotropic (appearing black under crossed polarizers) and then immediately applying a high-frequency pulse (to drive the cell into the twisted homogeneous light state) the cell can be driven between two optically very distinct alignments.

Optical waveguide characterization is a powerful method for accurately determining the director structure inside a liquid crystal cell [5,6]. A recent variation on the standard fully-leaky guided-mode technique allows the method's sensitivity to small changes in the director structure to be maintained whilst optical data is collected on a sub-millisecond timescale [7]. This method is ideal for studying the evolution of the dynamics of a CHAN cell on the application of a multiple-frequency pulse, allowing the complex director reorientation process to be examined in detail. It has been used here to study the complex dynamic processes involved in the switching of a CHAN cell

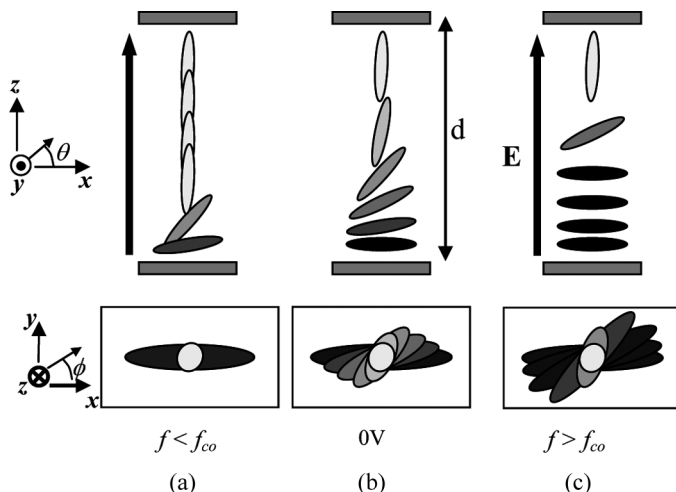


**FIGURE 1** Schematic diagram of the chiral HAN dual-frequency liquid crystal cell viewed in the  $x$ - $z$  and  $x$ - $y$  planes with (a) low-frequency high-voltage applied; (b)  $0V$  applied and (c) high-frequency high-voltage applied.

from  $0V$  to homeotropic alignment and then to a twisted-homogeneous structure. The results are compared to theoretical profiles generated using a nematodynamics model which incorporates a simple dual-frequency Debye-type model to describe the dielectric dispersion of the material.

## II. EXPERIMENT

A hybrid cell of thickness  $4.94\mu\text{m}$  was constructed using Indium Tin Oxide (ITO) coated low-index ( $n = 1.52$ ) glass. One substrate was coated with a rubbed polyimide to produce homogeneous alignment whilst the other was treated with a homeotropically aligning polyimide. The cell was then spaced using  $5\mu\text{m}$  glass beads dispersed in a UV curing glue along the edges. A non-chiral nematic dual-frequency liquid crystal MLC-2048 (Merck KGa) was doped with 1.05% CB15 (Merck, KGa) by weight to produce a pitch of around  $12.7\mu\text{m}$  and then introduced into the cell by capillary action. A good monodomain was produced which showed no extinction in transmission when rotated in the  $x$ - $y$  plane between crossed polarizers, demonstrating the presence of a cholesteric pitch.

The CHAN cell was refractive index-matched between two  $n = 1.52$   $60^\circ$  prisms and mounted at the centre of the time-resolved FLGM set-up [7]. Optical data was collected on a  $2\mu\text{s}$  timescale and synchronised

with the application of a multiple-frequency voltage pulse applied along the  $z$ -axis of the cell. The pulse used was composed of a sinusoidal voltage of  $7 V_{\text{rms}}$  at 2 kHz for 20 ms immediately followed by one of  $7 V_{\text{rms}}$  at 64 kHz for 80 ms.

Once obtained, the optical data for selected time-steps were fitted using a multi-layer optics model based on a  $4 \times 4$  Berreman matrix [8] and a least-squares fitting procedure. In this model the optical permittivities, absorptivities and the layer thicknesses of the ITO, homogeneous polyimide, homeotropic polyimide and liquid crystal were used as fitting parameters, along with the twist,  $\phi$  (measured anti-clockwise from the  $x$ -axis in the  $x$ - $y$  plane) and tilt,  $\theta$  (measured from the substrate) of the director orientation through the cell, described in both cases using second-order Bezier curves.

### III. RESULTS AND ANALYSIS

To avoid complications encountered when the director becomes homeotropic causing the twist angle to be undefined the twist and tilt profiles measured and produced from the fitting procedure were converted into the  $n_x$ ,  $n_y$  and  $n_z$  components of the director (unit vector  $\mathbf{n}$ ). These were defined as  $n_x = \cos \theta \cos \phi$ ,  $n_y = \cos \theta \sin \phi$  and  $n_z = \sin \theta$ .

Figure 2 shows the measured  $n_x$ ,  $n_y$  and  $n_z$  components at points  $1 \mu\text{m}$ ,  $2 \mu\text{m}$ ,  $3 \mu\text{m}$  and  $4 \mu\text{m}$  through the cell plotted as a function of time. As the electric field is applied solely along the  $z$ -axis the initial response of the cell is dominated by the response of the tilt,  $n_z$ . The twist reorientation (manifest in  $n_x$  and  $n_y$ ) is a secondary response on a much longer timescale due to no dielectric torque component acting in the plane of the twist. This response is dictated by the visco-elastic forces in the system, as discussed in detail later.

The variation of the director profile during the dual-frequency switching of the cell can be modelled using the Leslie-Ericksen-Parodi theory [9,10] to model the switch-on of the CHAN cell from 0 V to the twisted-homeotropic state initially using the low frequency value for  $\Delta\epsilon$  in the model. At the time when the frequency is switched (20 ms), the value of  $\Delta\epsilon$  used in the simulation is switched to the high-frequency value (assuming an instantaneous response to the change in frequency) and the switch-off director profile can be calculated.

The approach used here is based on work by Van Doorn [11] and the nematodynamic theory and the iterative approach used has been adapted to include variation in both twist and tilt, as presented in previous work [12]. For a CHAN cell, the evolution of both twist and tilt must be considered along with a coupling between the two, thus dynamic equations for  $n_x$ ,  $n_y$  and  $n_z$  are required. The modelling

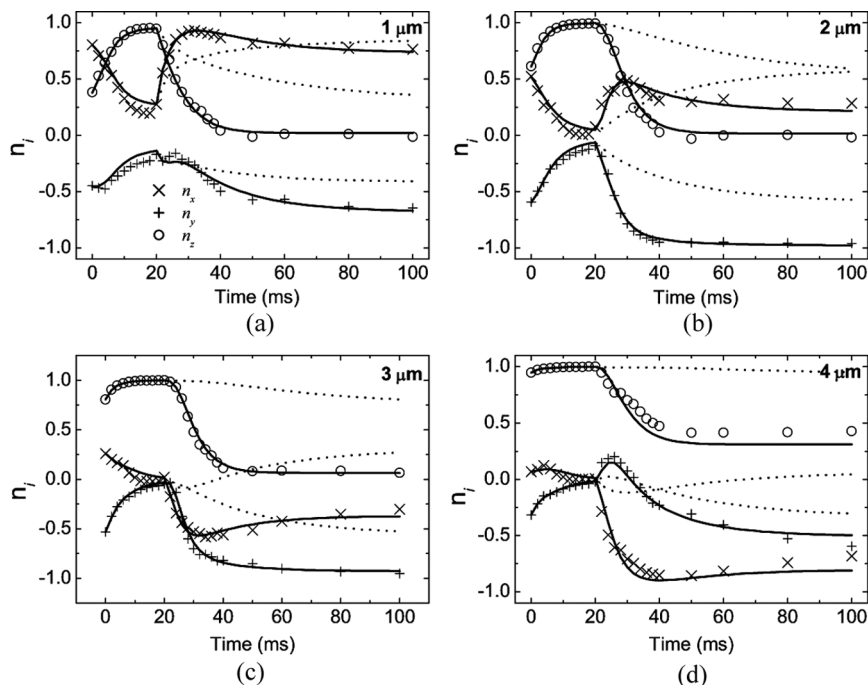


**FIGURE 2** Comparison of measured (symbols) and modelled (lines) of the time evolution of  $n_x$ ,  $n_y$  and  $n_z$  at points (a)  $1 \mu\text{m}$ ; (b)  $2 \mu\text{m}$ ; (c)  $3 \mu\text{m}$  and (d)  $4 \mu\text{m}$  through the cell. A low frequency field (2 kHz) is applied between  $t = 0$  and  $t = 20$  ms and a high frequency field (64 kHz) is applied between  $t = 20$  ms and  $t = 100$  ms. The values of the physical constants used are stated in the text. The dotted lines show the modelled natural relaxation of the cell if the voltage was switched to zero at  $t = 20$  ms.

process involves taking an initial static director profile and then using the Ericksen-Leslie-Parodi theory to determine the rate of change of the  $x$ -,  $y$ - and  $z$ -components of the director with time and using the Cranks-Nicholson method [13] to determine the director profile at the required times during the dynamic response of the cell. In the model used a Debye model was included to describe the dielectric dispersion of the material [14], allowing the frequency, rather than the actual dielectric anisotropy, to be used as an input parameter. This allowed the phase and amplitude of the time-varying field within the cell to be calculated and, for sufficiently low frequencies the director could be observed to follow the applied field.

The results of modelling the director response for the dual-frequency CHAN cell are shown as the solid lines in Figure 2.

The coefficients used in the modelling are  $k_{11} = 16.7 (\pm 1)$  pN,  $k_{22} = 10.0 (\pm 2)$  pN,  $k_{33} = 20.9 (\pm 1)$  pN and pitch =  $13.0 (\pm 1)$   $\mu\text{m}$ . The dielectric anisotropies used are  $\Delta\epsilon(2\text{ kHz}) = 2.6 (\pm 0.1)$  and  $\Delta\epsilon(64\text{ Hz}) = -2.3 (\pm 0.1)$  and the Miesowicz viscosity coefficients (defined using the Helfrich notation) used are  $\gamma_1 = 0.30 (\pm 0.02)$  Pas,  $\eta_1 = 0.33 (\pm 0.02)$  Pas,  $\eta_2 = 0.055 (\pm 0.02)$  Pas,  $\eta_3 = 0.085 (\pm 0.02)$  Pas and  $\eta_{12} = -0.01 (\pm 0.01)$  Pas.

The fits presented were obtained by manually adjusting these parameters in the nematodynamics model until a reasonable agreement was obtained with the director evolution at the four selected points in the cell. During this fitting procedure the influence of certain parameters on the form of the dynamic response of the cell were observed. The ratio  $\eta_2/\eta_3$  was found to influence the form of the peak that occurs in the  $n_y$  component towards the homeotropic surface (at  $\sim 4\text{ }\mu\text{m}$ ) immediately after the frequency is switched, whereas towards the centre of the cell (around  $2\text{ }\mu\text{m}$  and  $3\text{ }\mu\text{m}$ ) the rate of change of  $n_x$  after the application of the 64 kHz pulse is sensitive to the value of  $k_{22}$ . As in the case of a non-twisted HAN cell the final value of  $n_z$  at the end of each pulse section is dictated by the dielectric anisotropy of the material at 2 kHz and 64 kHz and the form of the reorientation is dominated by the rotational viscosity,  $\gamma_1$ . Varying the other viscosity coefficients by  $\pm 50\%$  (whilst obeying the inequalities governing the relative values that these coefficients can take [15]) had a negligible effect on the  $n_z$  profiles, hence the relatively large uncertainties in the figures quoted. The slight discrepancies between the measured and modelled variations of  $n_i$  with time can be partially attributed to the rigid anchoring approximation used in the dynamics model. In addition, the measured director components were obtained by using a mathematical curve (Bezier), rather than a physical model, to approximate the form of the director profile through the cell.

Using a projection onto the  $x$ - $y$  plane, Figure 3 illustrates a backflow effect that is produced when the frequency of the applied field is switched. At the end of the first frequency pulse, the cell is mainly homeotropically aligned (hence the twist is undefined) and the entire switch-on reorientation during this first 20 ms of the sequence is contained in the lower-right quadrant of the diagram. On application of the high-frequency section of the pulse however,  $n_y$  immediately becomes positive for around 10 ms before switching back to negative for the remainder of the pulse duration, whilst  $n_x$  switches to negative immediately and continues to increase in magnitude throughout the high-frequency pulse duration. Physically, this transition must be achieved by the director “falling backwards”, with the twist, measured clockwise from the  $x$ -axis, instantly increasing by around  $180^\circ$



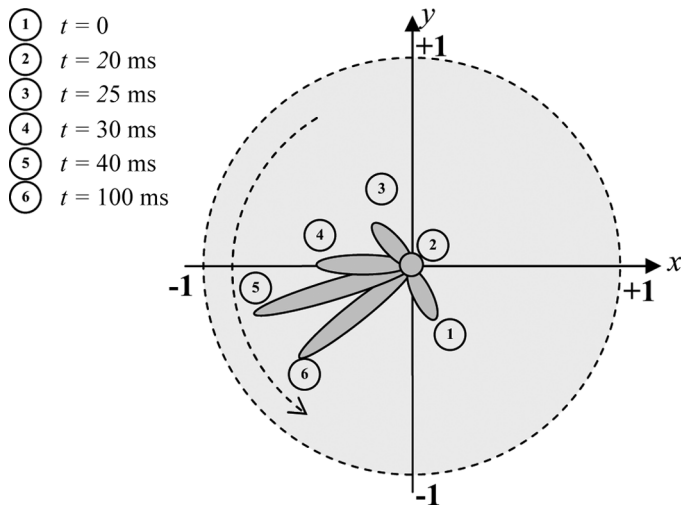


**FIGURE 3** Schematic representation of the motion of the director, projected onto the  $x$ - $y$  plane for switching a dual-frequency CHAN cell into homeotropic alignment (0 to 20 ms) and then driving it into the twisted nematic state using a high-frequency pulse.

at this point in the cell. The director is then driven down towards the substrate by the action of the applied field whilst simultaneously the twist reduces in magnitude as the visco-elastic forces draw the cell back into its naturally twisted equilibrium state. This can clearly be seen in Figure 4 which shows the complete evolution of the modelled tilt and twist profiles during the switching processes. Figure 4(d) shows an initial jump in the twist of  $180^\circ$  on application of the high-frequency, whilst Figure 4(c) demonstrates an oscillation in the tilt (measured from the  $x$ - $y$  plane) corresponding to the over-rotation of the director. On removal of the field producing the homeotropic alignment the splay-bend elastic torque in the bulk of the cell induces a rapid rotation towards homogeneous alignment, which induces a shear flow in both the  $x$ - and  $y$ - directions due to the twist distortion. Once the director has started to over-rotate the action of the high-frequency field causes the director to continue in that direction and so the equilibrium state is achieved through the director minimising the twist free-energy.

The influence of the effect of driving the director into homogeneous alignment on the backflow can be seen when it is compared to modelling of the un-driven natural relaxation of the cell when the cell is switched to homeotropic and the voltage is then removed. The dotted

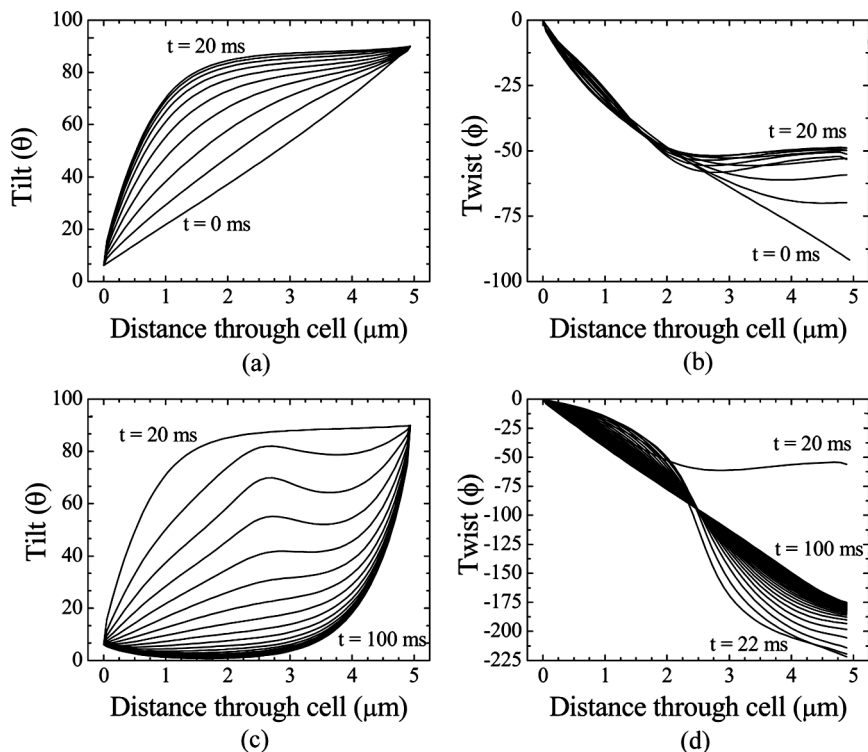


**FIGURE 4** Modelled evolution of the twist and tilt profiles (in 2 ms steps) of the director with time during the low-frequency switching to the homeotropic state ((a) and (b)) and the high-frequency switching to the twisted homogeneous alignment ((c) and (d)).

lines in Figure 2 show this effect, using the same parameters as in the previous modelling. In the natural relaxation case a very small amount of back-flow occurs on removal of the voltage causing the director to over-rotate, adding an extra  $180^\circ$  to the twist, but due to the director remaining close to the homeotropic state throughout (due to its proximity to the homeotropic substrate) this twist is relatively insignificant as regards its optical and elastic effects.

The values of the splay and bend elastic coefficients used in the modelling show reasonable agreement with the measured values of  $k_{11} = 15 (\pm 1)$  pN and  $k_{33} = 20 (\pm 1)$  pN obtained from Fréedericksz transition measurements on pure MLC-2048-000 at  $25^\circ\text{C}$ , with the discrepancies between the two likely to be due to the influence of the chiral dopant material on the elastic constants and the slight

temperature difference. The measured value of  $k_{22}$  appears high when compared to values for other nematic liquid crystals, but the ratio of the bend and twist coefficients measured here ( $k_{33}/k_{22} = 2.09$ ) is reasonable for a nematic material.

## IV. CONCLUSION

By using a chirally doped dual-frequency nematic liquid crystal in a hybrid aligned structure the director can be driven between homeotropic and twisted homogeneous alignment. Applying a multiple frequency pulse to the cell drives the director between the two states and a new form of backflow occurs when the frequency is switched from below to above the cross-over frequency of the material. This arises initially due to the over-rotation of the tilt close to the homeotropic surface due to a coupling between rotation and flow. It is then driven further by the combined effect of the negative dielectric anisotropy of the material at high frequencies and the pitch induced by the chiral dopant. The measured response of the cell shows good agreement with theoretical profiles generated using the Leslie-Ericksen-Parodi theory with flow in two dimensions. In this study the gain in response time achieved by the fast switching to the homogeneous state is compromised by the slow un-driven response of the twist, but with the use of a dual-frequency with optimised elastic and viscosity coefficients, such a structure may be suitable for use in a liquid crystal display.

## REFERENCES

- [1] Schadt, M. (1997). *Annu. Rev. Mater. Sci.*, 27, 305.
- [2] Raynes, E. P. & Shanks, I. (1974). *Electron. Lett.*, 10, 114.
- [3] Jewell, S. A. & Sambles, J. R. (2004). *Appl. Phys. Lett.*, 84, 46.
- [4] Lewis, M. R. & Wiltshire, M. C. K. (1987). *Appl. Phys. Lett.*, 51, 1197.
- [5] Yang, F. Z. & Sambles, J. R. (1999). *J. Opt. Soc. Am. B*, 16, 488.
- [6] Jewell, S. A. & Sambles, J. R. (2002). *J. Appl. Phys.*, 92, 19.
- [7] Jewell, S. A., Taphouse, T. S., & Sambles, J. R. (2005). *Appl. Phys. Lett.*, 87, 021106.
- [8] Ko, D. Y. K. & Sambles, J. R. (1988). *J. Opt. Soc. Am. A*, 5, 1863.
- [9] Ericksen, J. L. (1962). *Arch. Ration. Mech. Anal.*, 9, 371.
- [10] Leslie, F. M. (1966). *Q. J. Mech. Appl. Math.*, 19, 357.
- [11] Van Doorn, C. Z. (1975). *J. Appl. Phys.*, 46, 3738.
- [12] Jewell, S. A. & Sambles, J. R. (2006). *Phys. Rev. E*, 73, 011706.
- [13] Press, W. H., et. al. (1992). *Numerical Recipes in Fortran: The Art of Scientific Computing*, 2nd ed., Cambridge University Press: Cambridge.
- [14] Jewell, S. A. & Sambles, J. R. (2005). *Optics Express*, 13, 2627.
- [15] Stewart, I. W. (2004). *The Static and Dynamic Continuum Theory for Liquid Crystals*, Taylor and Francis: London.